



CONSTITUTIVE PARAMETER MEASUREMENTS  
USING THE SCATTERING TECHNIQUE

Jonathan D. Young

The Ohio State University

**ElectroScience Laboratory**

(formerly Antenna Laboratory)

Department of Electrical Engineering  
Columbus, Ohio 43212

TECHNICAL REPORT 1903-4  
6 February 1967

Contract NSR-36-008-027

National Aeronautics and Space Administration  
Office of Grants and Research Contracts  
Washington, D.C. 20546

FACILITY FORM 602

N67-18548  
(ACCESSION NUMBER)  
32  
(PAGES)  
CR 82015  
(NASA CR OR TMX OR AD NUMBER)

(THRU)  
(CODE)  
07  
(CATEGORY)

## NOTICES

When Government drawings, specifications, or other data are used for any purpose other than in connection with a definitely related Government procurement operation, the United States Government thereby incurs no responsibility nor any obligation whatsoever, and the fact that the Government may have formulated, furnished, or in any way supplied the said drawings, specifications, or other data, is not to be regarded by implication or otherwise as in any manner licensing the holder or any other person or corporation, or conveying any rights or permission to manufacture, use, or sell any patented invention that may in any way be related thereto.

The Government has the right to reproduce, use, and distribute this report for governmental purposes in accordance with the grant under which the report was produced. To protect the proprietary interests of the grantor and to avoid jeopardy of its obligations to the Government, the report may not be released for non-governmental use such as might constitute general publication without the express prior consent of The Ohio State University Research Foundation.

REPORT  
by  
The Ohio State University ElectroScience Laboratory  
(Formerly the Antenna Laboratory)  
COLUMBUS, OHIO 43212

Sponsor                      National Aeronautics and Space Administration  
                                 Office of Grants and Research Contracts  
                                 Washington, D.C. 20546

Contract Number          NSR-36-008-027

Investigation of            Radar and Microwave Radiometric  
                                 Techniques for Geoscience Experiments

Subject of Report          Constitutive Parameter Measurements  
                                 Using the Scattering Technique

Submitted by                Jonathan D. Young  
                                 ElectroScience Laboratory  
                                 Department of Electrical Engineering

Date                           6 February 1967

## ABSTRACT

A system has been constructed in order to evaluate the practicality of the scattering technique for measuring the constitutive parameters,  $\mu$  and  $\epsilon$ , of materials. Measurement data have been obtained for samples having a wide range of parameter values. Experimental results and a system error analysis are used to predict feasible accuracy for this technique.

## TABLE OF CONTENTS

	Page
I. INTRODUCTION	1
II. THEORY	2
III. THE MEASUREMENT SYSTEM	7
IV. RESULTS	10
V. SUMMARY AND CONCLUSIONS	24
APPENDIX A - CIRCUIT COMPONENTS OF THE MEASUREMENT SYSTEM	26
REFERENCES	27

# CONSTITUTIVE PARAMETER MEASUREMENTS USING THE SCATTERING TECHNIQUE

## I. INTRODUCTION

The problem of measuring the complex constitutive parameters  $\mu^*$  and  $\epsilon^*$  of materials at microwave frequencies is neither recent nor without many solutions. However, recent interest in and use of more complex materials has extended the range of parameter values for which accurate measurements are required, and has emphasized some shortcomings in the conventional techniques; for example, exceedingly small machining tolerances become necessary to maintain accuracy. Also, the properties measured by present methods are often not sufficiently sensitive to parameter variation in these new regions of interest. Finally, the solution of multiple transcendental equations is normally required to translate experimental data into constitutive parameters. Thus, there is a need for detailed consideration of new methods for measuring the electromagnetic properties of materials at microwave frequencies.

One new proposal for measuring constitutive parameters might be called the scattering method. This technique uses measurements of bistatic electromagnetic scattering from small spherical samples in free space to determine  $\mu^*$  and  $\epsilon^*$ . The method has several appealing qualities. Although the machining process may be more difficult for some materials, tolerance problems are lessened. The equations relating experimental data to constitutive parameters, while extremely complicated for spheres of arbitrary size, can be greatly simplified when, as in this technique, the spheres are small. Some quick and convenient methods of solving them have been devised. Furthermore, the bistatic scattering measurements used in this method are already common and well understood.

The scattering method also has some inherent problems. The basic assumptions in this technique are that only the dipole spherical scattering modes are significant, and furthermore that these may be approximated by simple equations. Spheres which fit these assumptions are extremely small, on the order of  $0.02\lambda$  diameter or less, and their amounts of scattered radiation are correspondingly minute, making measurement difficult. It will also become evident that extreme measurement accuracy is required for materials with high values of  $\mu^*$  and  $\epsilon^*$ . Because of these considerations, serious questions concerning the practicability of this method are raised.

One partial solution to this measurement problem has already been proposed. A more complicated expression for electromagnetic scattering which is valid for larger spheres has been developed by Yu.<sup>2</sup> The cost of this extension is that twice as many measurements are required.

In this report, only the experimental problem is considered. The primary objective is to determine if the required small sphere measurements can be obtained and, if so, with what accuracy, applicability, and difficulty. Results of this report also indicate when the increased difficulty of the extended theory technique is worthwhile.

In the second section, the theory of this technique is briefly reviewed and the required experimental measurements are specified. A system for making these measurements is discussed in the third section. Some data on specific materials are presented in the fourth section, and a system error analysis and suggested improvements are discussed. Finally, some conclusions are reached concerning the practicability and implementation of this method.

## II. THEORY

The theoretical bistatic scattering from spheres in general is very complex, being expressed by a pair of infinite series.<sup>1</sup> However, if certain limitations are placed on sphere characteristics and the method of measurement, the theoretical solution can be simplified to yield a rather direct relationship between the constitutive parameters and measureable scattering parameters. This theoretical development<sup>2</sup> may be quickly summarized.

Starting with the general scattering theory several assumptions are made as follows:

1. A plane-wave is incident upon the sphere.
2. The sphere material is homogeneous and isotropic.
3. All spheres satisfy the relation  $k_0 a \leq 0.2$ , where  $a$  is the sphere radius and  $k_0$  is the free-space wave number. By definition these are dipole spheres.
4. Measurements are to be made in the E and H planes at the bistatic angle of  $90^\circ$  where geometry is as shown in Fig. 1.

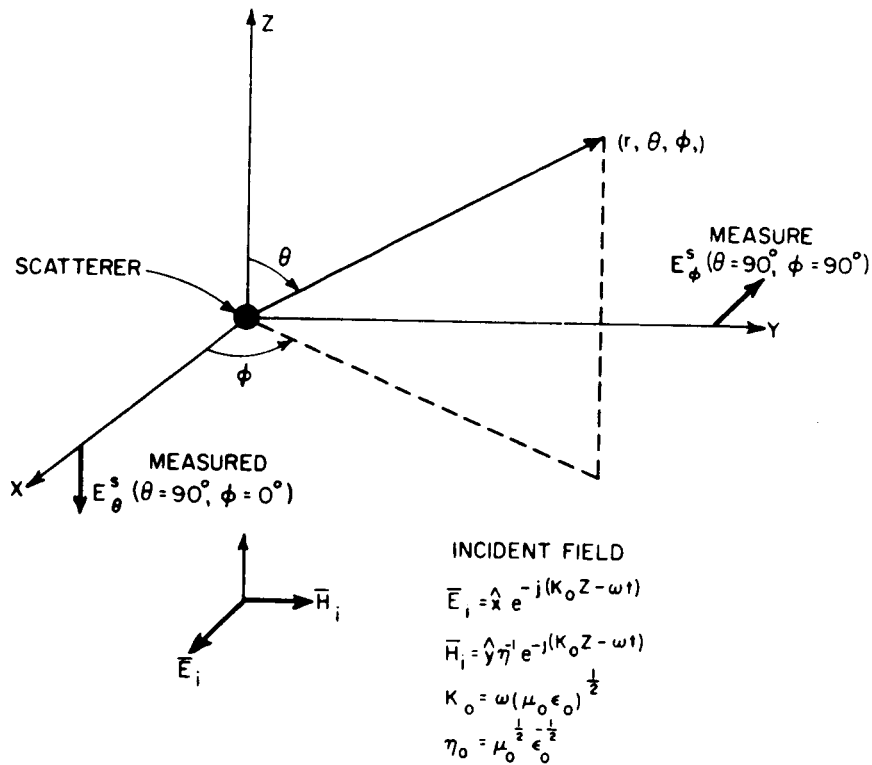


Fig. 1. Diagram of necessary scattering measurements.

Then for the above specified conditions the scattered fields for a sphere can be obtained with better than 1% accuracy at a given distance  $\rho_0$  as

$$(1) \quad E_\theta \left( \rho_0, \theta = \frac{\pi}{2}, \phi = 0 \right) = (j\rho_0)^{-1} \frac{3}{2} \left[ a_1^c(\sigma_0) \frac{\eta_r^{-1} X_1(\nu_r \sigma_0) - A_1(\sigma_0)}{\eta_r^{-1} X_1(\nu_r \sigma_0) - B_1(\sigma_0)} \right] \zeta_1(\rho_0)$$

and

$$(2) \quad E_\phi \left( \rho_0, \theta = \frac{\pi}{2}, \phi = \frac{\pi}{2} \right) = - (j\rho_0)^{-1} \frac{3}{2} \left[ b_1^c(\sigma_0) \frac{\eta_r X_1(\nu_r \sigma_0) - A_1(\sigma_0)}{\eta_r X_1(\nu_r \sigma_0) - B_1(\sigma_0)} \right] \zeta_1'(\rho_0) .$$

For a perfectly conducting sphere of the same size, the corresponding scattered fields can be written as

$$(3) \quad E_{\theta}^c \left( \rho_0, \theta = \frac{\pi}{2}, \phi = 0 \right) = (j\rho_0)^{-1} \frac{3}{2} a_1^c(\sigma_0) \zeta_1(\rho_0)$$

and

$$(4) \quad E_{\phi}^c \left( \rho_0, \theta = \frac{\pi}{2}, \phi = \frac{\pi}{2} \right) = - (j\rho_0)^{-1} \frac{3}{2} b_1^c(\sigma_0) \zeta_1'(\rho_0) .$$

In these equations, the parameters are

$$\sigma_0 = k_0 a = 2\pi \frac{a}{\lambda_0} = 2\pi \frac{\text{SPHERE RADIUS}}{\text{FREE SPACE WAVELENGTH}} ,$$

$$\eta_r = \sqrt{\frac{\mu_r}{\epsilon_r}} \quad \nu_r = \frac{1}{\sqrt{\mu_r \epsilon_r}} ,$$

$$a_1^c(\sigma_0) = - \frac{j_1(\sigma_0)}{h_1^{(2)}(\sigma_0)} ,$$

$$b_1^c(\sigma_0) = - \frac{2j_1(\sigma_0) - \sigma_0 j_2(\sigma_0)}{2 h_1^{(2)}(\sigma_0) - \sigma_0 h_2^{(2)}(\sigma_0)} ,$$

$$X_1(\nu_r \sigma_0) = \frac{2}{\nu_r \sigma_0} - \frac{j_2(\nu_r \sigma_0)}{j_1(\nu_r \sigma_0)} ,$$

$$A_1(\sigma_0) = \frac{2}{\sigma_0} - \frac{j_2(\sigma_0)}{j_1(\sigma_0)} , \quad \text{and}$$

$$B_1(\sigma_0) = \frac{2}{\sigma_0} - \frac{h_2^{(2)}(\sigma_0)}{h_1^{(2)}(\sigma_0)} ,$$

where the  $j$ 's are spherical Bessel functions, the  $h$ 's are spherical Hankel functions, and dipole scattering only is considered.

The two sets of fields specified can be measured in the near-zone. Their ratios are

$$(5) \quad \gamma_{\theta} = \frac{E_{\theta}(\rho_0, \theta = \frac{\pi}{2}, \phi = 0)}{E_{\theta}^c(\rho_0, \theta = \frac{\pi}{2}, \phi = 0)} = \frac{\eta_r^{-1} X_1(\nu_r \sigma_0) - A_1(\sigma_0)}{\eta_r^{-1} X_1(\nu_r \sigma_0) - B_1(\sigma_0)}$$

and

$$(6) \quad \gamma_{\phi} = \frac{E_{\phi}(\rho_0, \theta = \frac{\pi}{2}, \phi = \frac{\pi}{2})}{E_{\phi}^c(\rho_0, \theta = \frac{\pi}{2}, \phi = \frac{\pi}{2})} = \frac{\eta_r^{-1} X_1^{-1}(\nu_r \sigma_0) - A_1^{-1}(\sigma_0)}{\eta_r^{-1} X_1^{-1}(\nu_r \sigma_0) - B_1^{-1}(\sigma_0)} .$$

With algebraic manipulation and simplification, the relationships between the unknown quantities,  $\eta_r$  and  $\nu_r$ , and the experimentally measured ratios,  $\gamma_{\theta}$  and  $\gamma_{\phi}$ , can be expressed as

$$(7) \quad \eta_r = + \sqrt{\frac{2c(1 - \gamma_{\theta})(1 - \gamma_{\phi})}{(2 + c\gamma_{\theta})(c + 2\gamma_{\phi})}}$$

and

$$(8) \quad X_1(\nu_r \sigma_0) = \frac{1}{\sigma_0} \sqrt{\frac{2c(2 + c\gamma_{\theta})(1 - \gamma_{\phi})}{(1 - \gamma_{\theta})(c + 2\gamma_{\phi})}} ,$$

where

$$c = (1 - \sigma_0^2) + j\sigma_0^3 \quad \text{with } \sigma_0 \leq 0.2 .$$

The solution to Eq. (7) is straightforward. For Eq. (8) a refractive index chart (shown in Fig. 2) has been constructed to facilitate finding the argument of  $X_1(\nu_r \sigma_0)$ , given the complex value of that function.

If the sample sphere satisfies the additional conditions that  $k_1 a \leq 0.31$ , where  $k_1$  is the wave number of the material, and  $\sigma_0 \leq 0.1$ , the relationship can be further simplified. For this case, the constitutive parameters are expressed directly as

$$(9) \quad \mu_r = 2 \frac{1 - \gamma_{\theta}}{2 + \gamma_{\theta}}$$

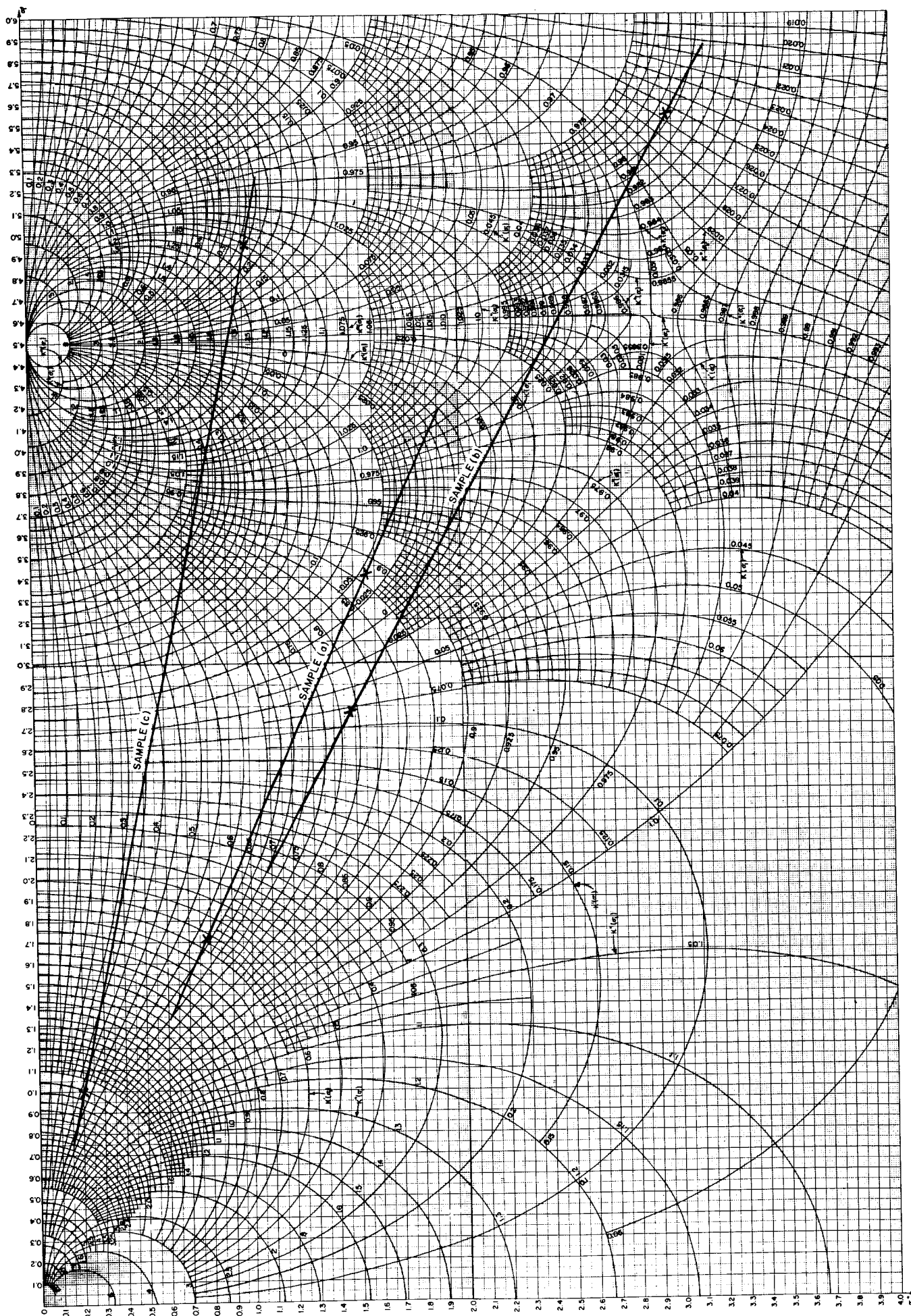


Fig. 2. Refractive index chart.

and

$$(10) \quad \epsilon_r = \frac{1 + 2\gamma_\phi}{1 - \gamma_\phi},$$

with  $k_1 a \leq 0.31$  and  $\sigma_0 \leq 0.1$ . Use of these relations for finding constitutive parameters from scattering measurements was first proposed by Moffatt.<sup>3</sup>

As can be seen, this theoretical development has not only determined the relationship between constitutive parameters and sphere bistatic scattering, but it has also specified the nature of the experiment to measure the scattering. Basically, a small sphere ( $k_0 a \leq 0.2$ ) must be illuminated by a plane wave and the magnitude and phase of its scattered field at two bistatic angles ( $\theta = 90^\circ$ ,  $\phi = 0^\circ$  and  $\theta = 90^\circ$ ,  $\phi = 90^\circ$ ) must be measured. The process is then repeated for a conducting sphere of the same size. If this experiment can be performed successfully and accurately for spheres of arbitrary materials, a new measurement method for constitutive parameters has indeed been developed.

As discussed by Yu,<sup>2</sup> a generalization of the theoretical relations to include the effects of quadrupole sphere scattering modes results in a valid but more complicated scattering method for measuring constitutive parameters of spheres with  $k_0 a \leq 1$ . This method requires two additional bistatic scattering measurements, one each in the E- and H-planes, at other bistatic angles. This method will be briefly discussed after and in relation to the simpler technique.

### III. THE MEASUREMENT SYSTEM

A typical system for measuring bistatic scattering uses two antennas spaced  $90^\circ$  apart in the far field of the target, as shown in Fig. 3. One antenna transmits energy to illuminate the target, and the other receives the scattered radiation. A nulling loop between transmitter and receiver is used to cancel direct radiation between the antennas and unwanted scattering from the target support and other nearby objects.

Thus, when a sample is being measured, there are actually three signal inputs to the receiver; i.e., Signal #1 - bistatic scattering from the sample, Signal #2 - unwanted signal, and Signal #3 - Null loop signal to cancel out Signal #2. Although the sum of Signals #2 and #3 is ostensibly zero, various external factors in any system of this type,

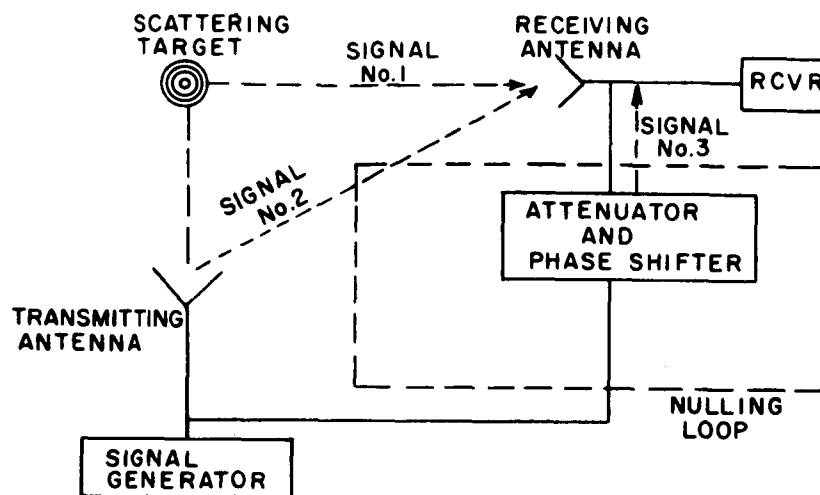


Fig. 3. Typical bistatic scattering range.

such as temperature change and mechanical vibrations, cause variations in the "null level" resulting from these two signals. The measurement error caused by this effect depends on both system stability with respect to external factors and on the relative magnitudes of the signals involved.

For example, assume that the magnitudes of signals #1 and #2 are equal, and that #3 initially completely cancels signal #2. Now if external "noise" is introduced to cause a 5% change in signal #2, the resulting "null level" shift could possibly cause a  $\pm 5\%$  error in the measurement of Signal #1. However, if the magnitude of the unwanted signal is 20 dB greater than the magnitude of signal #1, the same 5% change could cause a  $\pm 50\%$  error in measuring Signal #1.

It is therefore evident that design goals for this system are maximum possible stability and maximization of the ratio of signal scattered from the sample to unwanted signal. In terms of the antennas for this system, maximum coupling to the scatterer and minimum direct coupling between antennas are required.

The antenna system chosen for this application is shown in Fig. 4. Incident power is coupled onto a two-wire transmission line<sup>5</sup> and propagates in the T-line mode to the scatterer. The scatterer, located

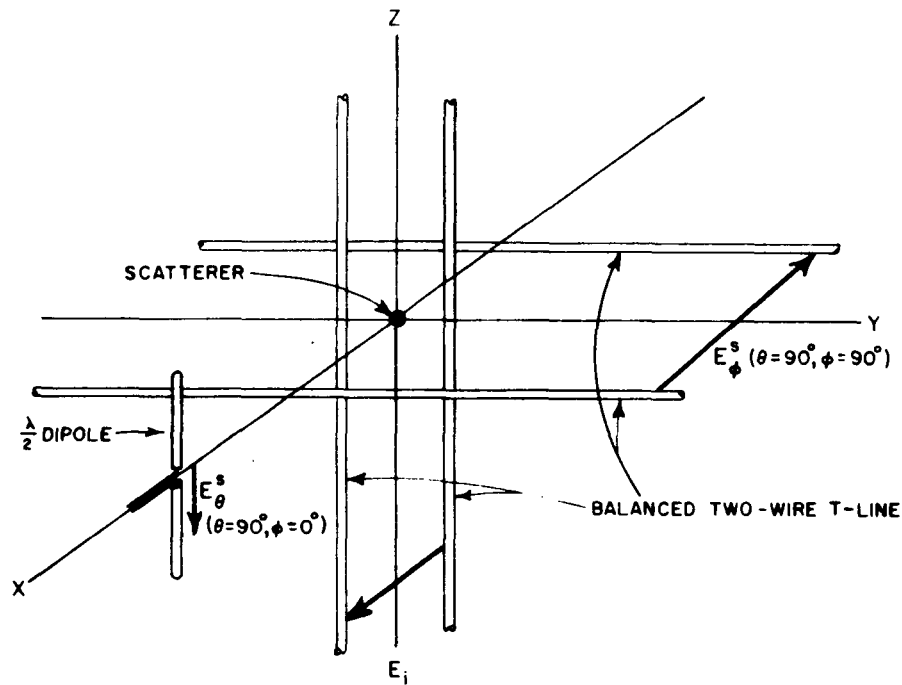


Fig. 4. Antenna orientation for scattering measurements.

symmetrically between the two wires, is illuminated by a TEM field with essentially constant field intensity. The scattered field in the direction  $(\theta = 90^\circ, \phi = 90^\circ)$  is coupled to another two-wire transmission line which acts as the receiving antenna. The scattered field in the direction  $(\theta = 90^\circ, \phi = 0^\circ)$  is received by a parasitic antenna array consisting of a dipole spaced optimally from the two wires of the transmitting T-line.

Using this system, the scattered power received from a  $\lambda_0/25$ -diameter conducting sphere in the direction  $(\theta = 90^\circ, \phi = 90^\circ)$  is 68 dB down from power input to the system, and in the direction  $(\theta = 90^\circ, \phi = 0^\circ)$  is 75 dB down from input power. Direct coupled power between the two transmission lines is 30 dB down from input power and coupling between transmission lines and dipole receiving antenna is 45 dB down from input power.

The  $6' \times 6' \times 6'$  anechoic chamber containing the system (shown in Figs. 5 and 6) is constructed of braced plywood, and lined with copper and 8"-thick sections of hairflex absorber. The measurement system is attached rigidly by clamp apparatus to this box. Stability of the enclosed system can be described as good. Satisfactory nulls can be maintained for periods of several minutes with proper care.

Considering the levels of scattered power and direct coupled power as stated heretofore, it is obvious that an accurate and stable nulling loop must be included in this system. A schematic diagram of all system circuitry, including the nulling loop, is shown in Fig. 7. This system used available components such as ordinary RG-8 coaxial cable. A complete specification of all components is in Appendix A. Unfortunately, the components were not particularly suited to this task. The null loop was difficult to adjust with the necessary accuracy and was very sensitive to mechanical disturbances. Also, a more powerful and more stable signal source would have been desirable. However, with present equipment, null levels 25 dB below the scattering from a  $\lambda_0/25$ -diameter conducting sphere can be obtained and maintained for several minutes.

The scheme for positioning the samples is shown in Fig. 8. Samples are lowered from the top through the styrofoam locating trough and into position, resting on the small styrofoam platform. Thus, the sample is not exactly in free space. However, the low dielectric constant of the locating apparatus and the nature of the measurement make the resulting error small.

#### IV. RESULTS

Measurements have been made on several sphere samples using the system discussed in the preceding section. These measurements are intended to show, in a general way, what difficulties are found in measuring small spheres, whether the method gives valid results, and what level of accuracy can be expected. Because of the experimental nature of this system and the less-than-satisfactory performance of some of its components, the measurement data do not portray optimum results for this measurement technique.

Figure 9 shows measured bistatic scattered power for several metal spheres. Since these spheres are in the Rayleigh region, a Rayleigh Law curve, normalized to the largest sphere, is also plotted. These measurements show that Rayleigh spheres can indeed be measured

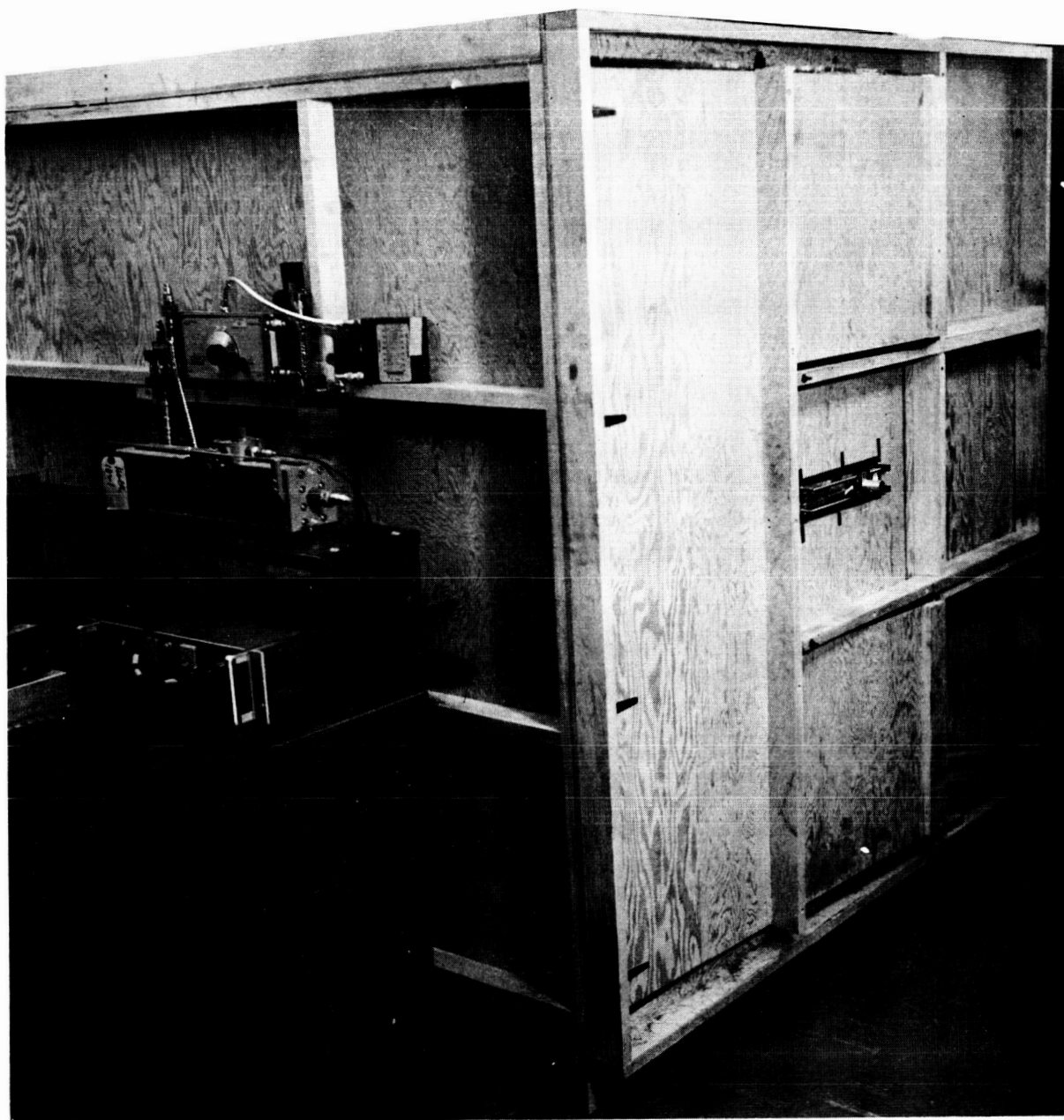


Fig. 5. Exterior view of scattering range.

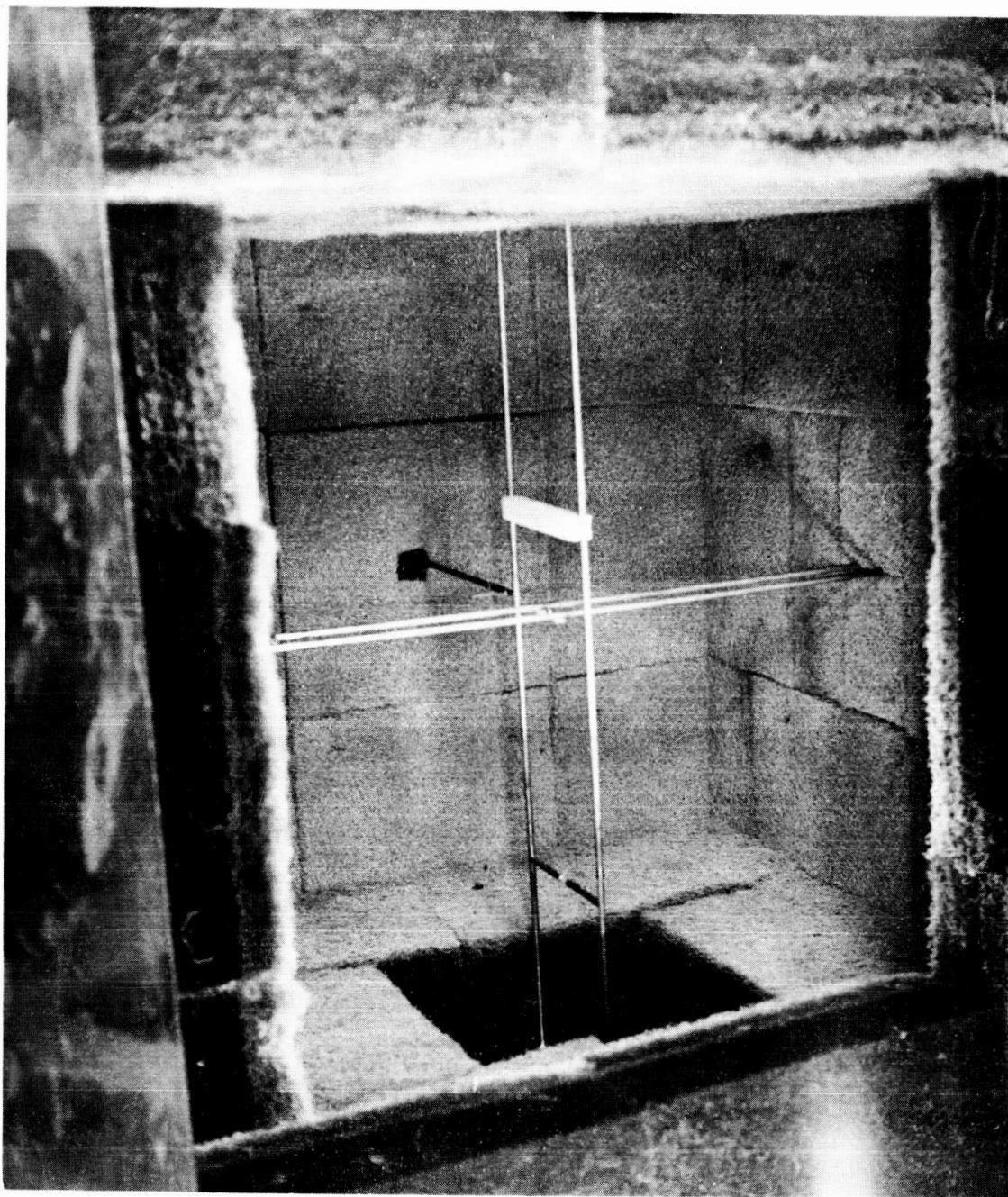


Fig. 6. Interior view of scattering range.

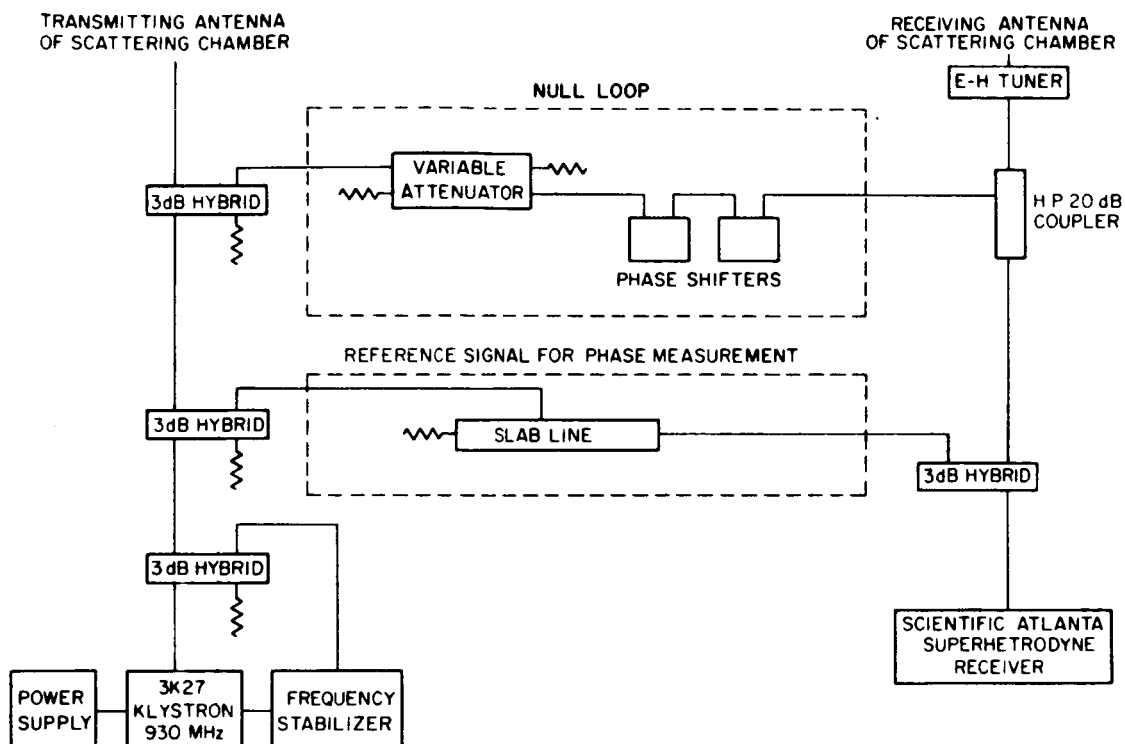


Fig. 7. Block diagram of exterior scattering range circuitry.

with good accuracy by a scattering range of this type, which in itself is a significant result. These measurements were made at the bistatic angle ( $\theta = 90^\circ$ ,  $\phi = 90^\circ$ ) with the dipole antenna, which is the less sensitive of the two receiving antennas.

Table I shows measured data on two samples of known dielectric constant, Teflon and Polystyrene. The simple relations were used for calculating  $|\epsilon_r|$  in this case. As can be seen, the average measurement value gives very accurate results. However, the spread of measurements could give values as much as 6% in error.

Table II shows measured data on seven sphere samples covering a wide range of constitutive parameter values; the samples were supplied by Emerson and Cuming, Inc. For samples C, E, and F, parameter values measured by Emerson and Cuming at a frequency of 8.6 GHz<sup>4</sup> are shown for comparison. Samples H, I, K, and L are

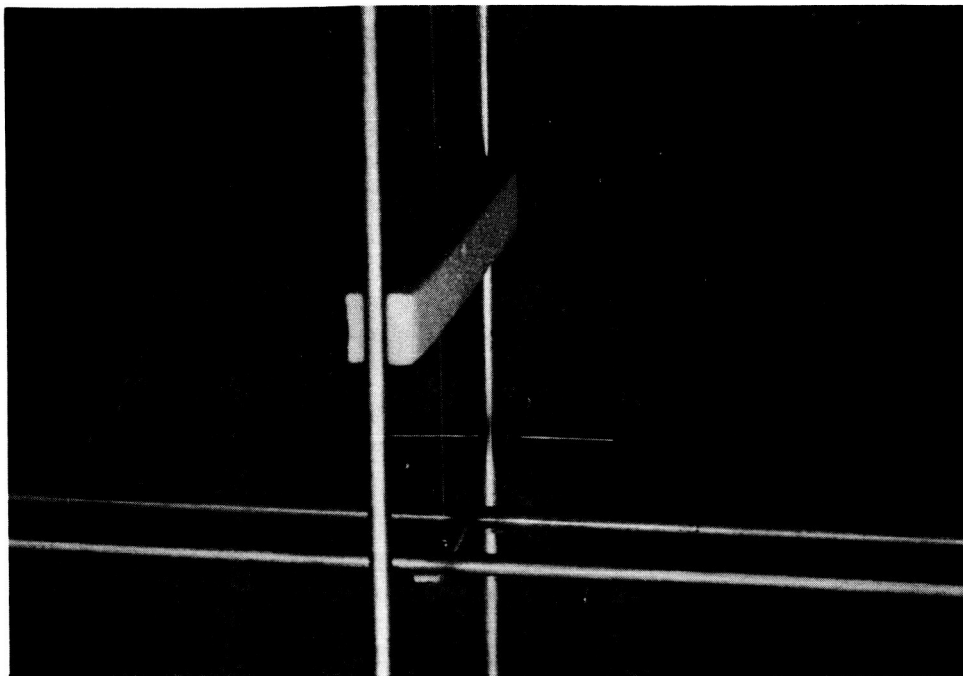


Fig. 8. Diagram of sample positioning scheme.

specimens of Eccosorb MF, Emerson and Cuming's line of waveguide absorber material. For these materials, nominal parameter values at a frequency of 1 GHz, as specified in Emerson and Cuming Technical Bulletin 8-2-6, are presented for comparison. For all of the materials in Table II, the absolutely correct parameters values at the measurement frequency are not known. Therefore, the accuracy of these measurements can only be estimated by noting data spread and by general comparison of parameter values.

After reviewing the experimental data it is evident that measurements can be obtained over virtually the entire range of constitutive parameters of interest. The data also seem to confirm the validity of the technique. But the accuracy obtainable from this method remains in question. This problem will now be considered based on the experimental data and simplified system analysis.

Experimental errors from this measurement system may be attributed to two basic sources. The first cause, which could be called recording error, is error in recording the amplitude and phase of the

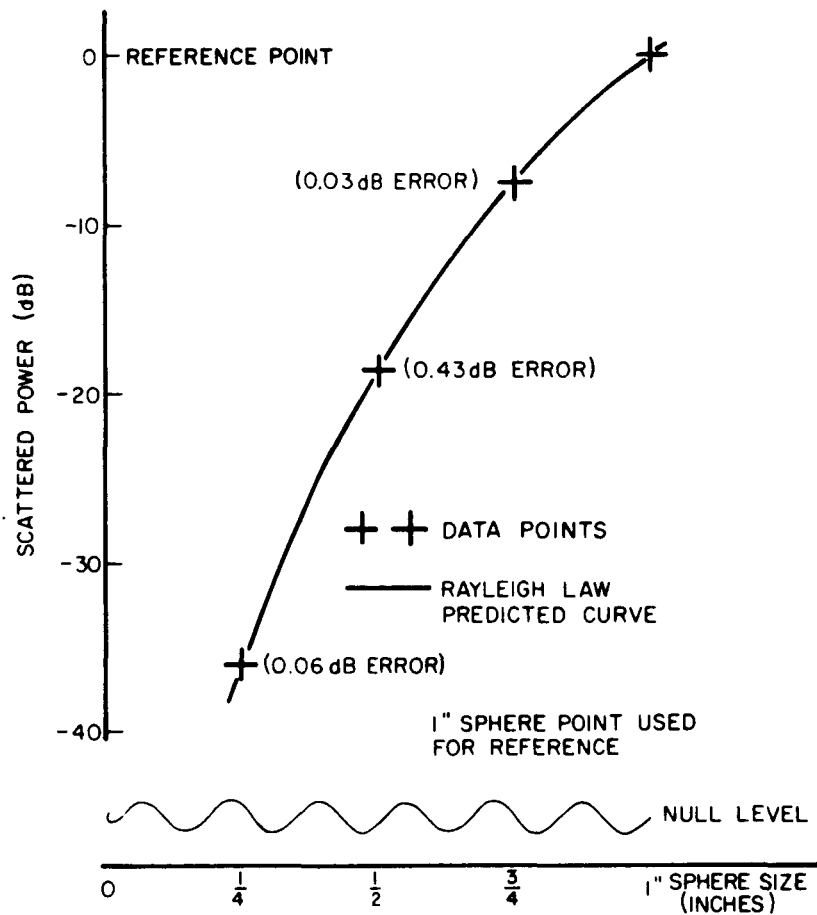


Fig. 9. Bistatic scattered power vs. sphere size for metal spheres.

TABLE I  
DIELECTRIC CONSTANT MEASUREMENTS

MATERIAL	NUMBER OF MEAS.	RELATIVE NULL LEVEL (dB)	MEASURED $ \gamma_\phi $		CALCULATED $ \epsilon_r $		CORRECT $ \epsilon_r $
			RANGE	AVERAGE	RANGE	AVERAGE	
TEFLON	5	20	.259 → .298	.273	2.05 → 2.27	2.12	2.10
POLYSTYRENE	5	20	.32 → .363	.339	2.41 → 2.71	2.54	2.55

TABLE II  
CONSTITUTIVE PARAMETER MEASUREMENTS

SAMPLE	NUMBER OF MEAS	RELATIVE NULL LEVEL (dB)	DATA SPREAD		AVERAGE VALUE		CALCULATED $\epsilon_r$			CALCULATED $\mu_r$		
			$\gamma_\phi$	$\gamma_\theta$	$\gamma_\phi$	$\gamma_\theta$	SIMPLE FORMULA	CHART METHOD	E & C	SIMPLE FORMULA	CHART METHOD	E & C
C	5	25	.872 → .967 1.1° → -3.3°		0.925 /-1.50°	0 (ASSUMED)	34.3-j11.7	29.4-j18.37	20.9-j.58			
E	5	24	.819 → .847 1.1° → -3.3°		0.833 /-1.1°	0 (ASSUMED)	15.8-j11.7	15.3-j1.57	9.61-j3.08			
F	5	25	.907 → .995 -1.1° → -5.6°		0.945 /-4.15°	0 (ASSUMED)	19.4-j26.45	19.95-j24.05	23.5-j10.1			
H	6	25	.590 → .680 2.2° → -3.3°	.348 → .413 172.1° → 178.8°	0.640 /-1.1°	0.386 /175.5°	6.34-j.29	6.36-j.269	5.5-j.275	1.72-j.078	1.70-j.061	1.6-j.0
I	6	24	.777 → .833 3.3° → -3.3°	.786 → .852 168.7° → 174.2°	0.805 /0°	0.815 /172.8°	13.4-j0	12.75+j.11	10-j.55	2.98-j.476	2.80-j.364	2.3-j0
K	4	25	.903 → 1.08 +2.2° → 0°	1.285 → 1.31 165.8° → 172.4°	0.98 /+1.1°	1.30 /168°	76.5+j74.5		22-j1.5	5.33-j2.75		4.0-j.52
L	12	25	.935 → 1.02 5.5° → -1.1°	1.57 → 1.625 160.2° → 167.9°	0.98 /1.66°	1.60 /167.5°	47+j70		23.5-j2.7	5.23-j6.57		4.8-j1.68

scattered signal as presented to the meters or measuring instruments. This would include device error as well as faulty readings. The second cause, which will be called system error, is the extraneous signal in the system output. This category would include random noise and also the error signal resulting from imperfect nulling of the system.

The error effects may be analyzed using a vector diagram. In Fig. 10, consider that the measured magnitude and phase of scattered signal from a sample sphere and corresponding metal sphere are represented by two vectors. The diagram is normalized so that the metal sphere signal,  $S_m$ , is the vector  $1 + j0$ . Then the sample scattered field vector,  $S_s$ , is equal to the ratio  $\gamma$ .

The system error may be represented as a small vector of random phase which is added to both signal vectors. The resulting locus of possible values for each sphere signal is the interior of a circle of specified radius which is centered at the tip of each vector  $S_m$  and  $S_s$ , as shown in Fig. 11. The radius is equal to the ratio of null signal level

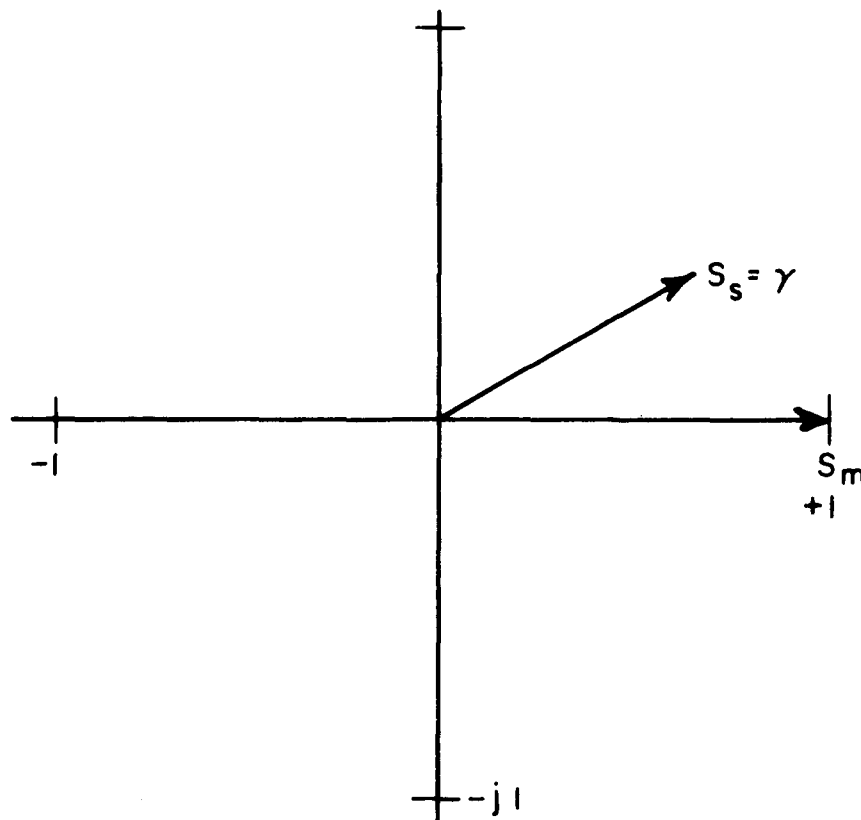


Fig. 10. Vector diagram representing scattered signals.

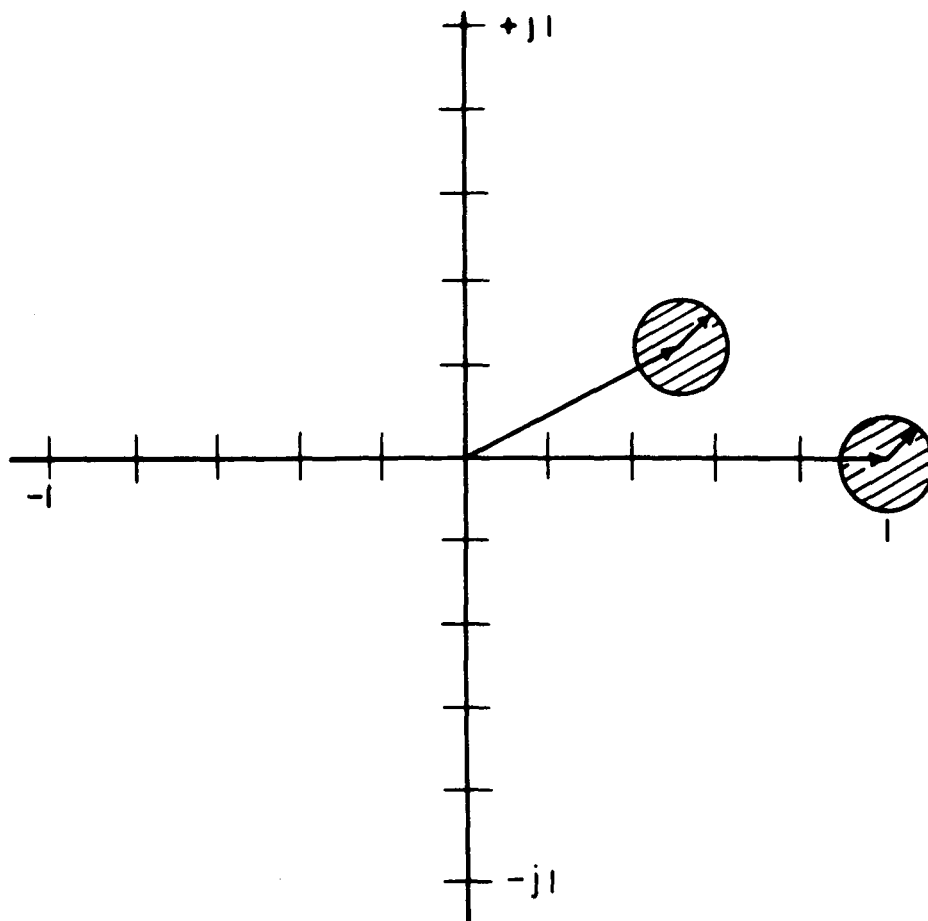


Fig. 11. Vector diagram representing effect of system error on scattered signals.

to metal sphere scattered signal level. This ratio of signal levels is therefore a figure of merit for a measurement system of this type.

Amplitude and phase recording errors cause a widening of the boundaries of the above circles by small amounts in the radial and phase direction, respectively. In the present system, recording errors are very small compared to system error. In other feasible systems, this relationship could always be obtained by buying measuring instruments of higher and higher quality. Therefore, recording error will be ignored henceforth in this analysis.

Because of variation of both vectors,  $S_m$  and  $S_s$ , the locus of possible values of  $\gamma$  is not clear from the diagram in Fig. 11. A simplifying assumption in this case is that the locus of possible values of  $\gamma$  is the interior of a circle centered at the tip of  $S_s$  with radius equal to twice the system relative null level, as shown in Fig. 12. This assumption gives a very conservative estimate for materials with relatively low parameter values.

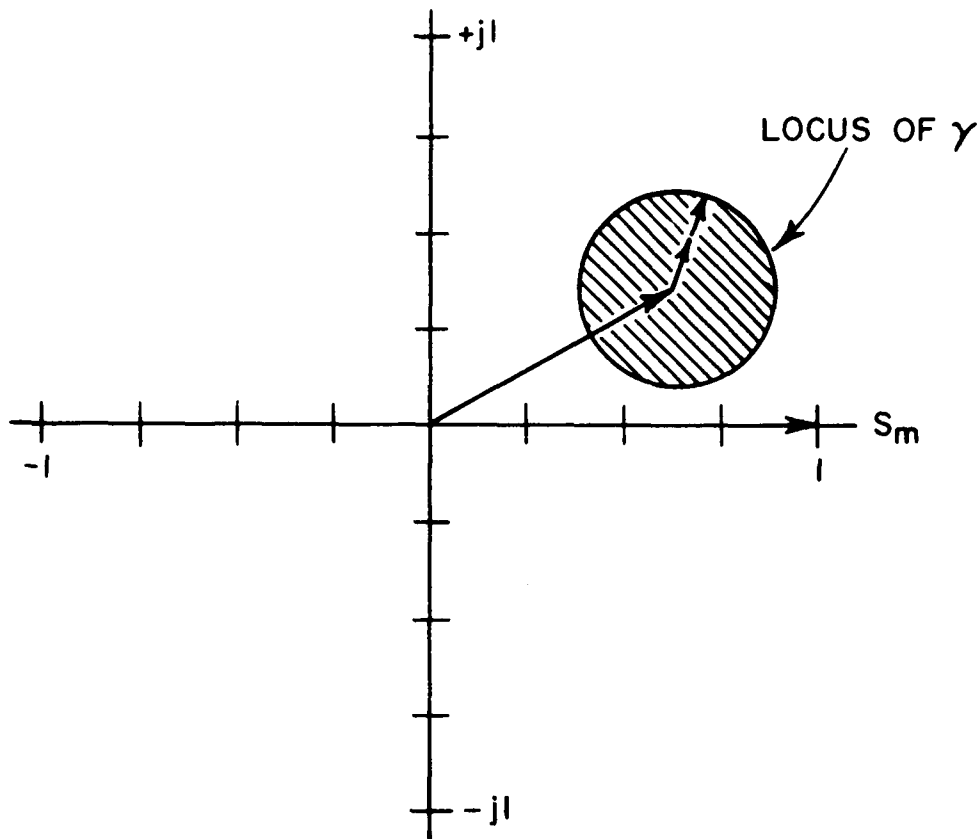


Fig. 12. Vector diagram representing approximate effect of system error on  $\gamma$ .

For the system in this report, the null level was about 26 dB down from the scattered signal from the  $\frac{1}{2}$ " metal reference sphere. Thus there was a possible error of  $0.1/\theta$ ,  $0 \leq \theta \leq 2\pi$ , in  $\gamma_\theta$  and  $\gamma_\phi$ . For comparison, systems with relative null levels of -36 dB, -46 dB, -56 dB, and -66 dB will also be considered. These systems would yield possible errors in  $\gamma_\theta$  and  $\gamma_\phi$  of  $0.032/\theta$ ,  $0.010/\theta$ ,  $0.0032/\theta$  and  $0.001/\theta$ , respectively. The simple relations (from Chapter 1) between  $\gamma_\theta$ ,  $\gamma_\phi$ ,  $\mu_r$ , and  $\epsilon_r$  were used to transform the locus of possible  $\gamma$  to an approximate locus of possible  $\mu_r$  and  $\epsilon_r$ . As will be seen, these loci are functions not only of relative null level, but also of the exact value of  $\mu_r$  and  $\epsilon_r$ .

Figure 13 shows the locus of possible  $\epsilon_r$  vs  $\epsilon_r$  and relative null level. Figure 14 shows the locus of possible  $\mu_r$  vs.  $\mu_r$  and relative null level. Notice that accuracy deteriorates rapidly as  $|\mu_r|$  or  $|\epsilon_r|$  and relative null level are increased. The characteristics also show that accurate measurements of loss tangent for low-loss materials would be very difficult. The measured data presented already indicate that the

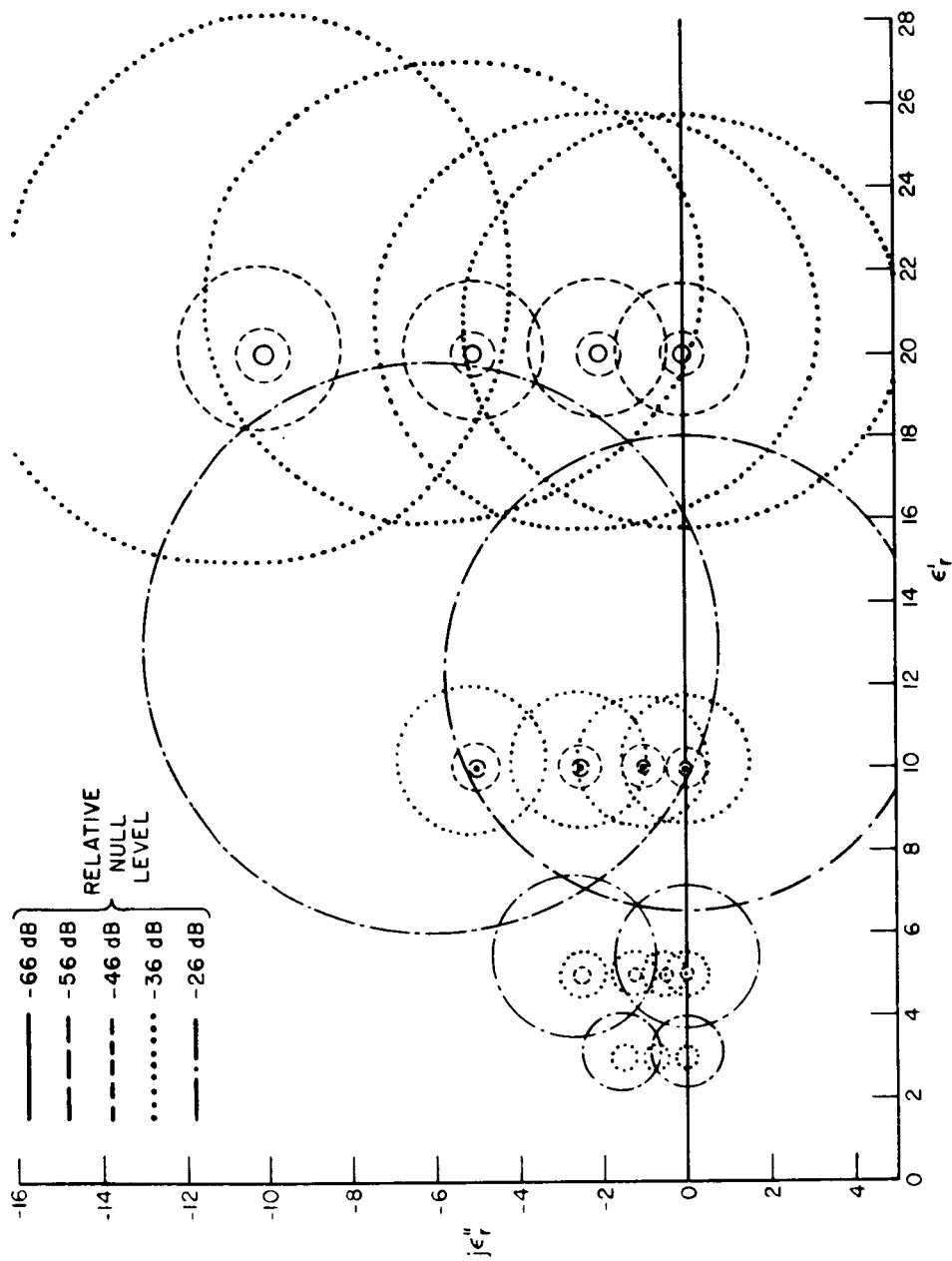


Fig. 13. Locus of possible measured  $\epsilon_r$  vs. correct  $\epsilon_r$  and relative null level.

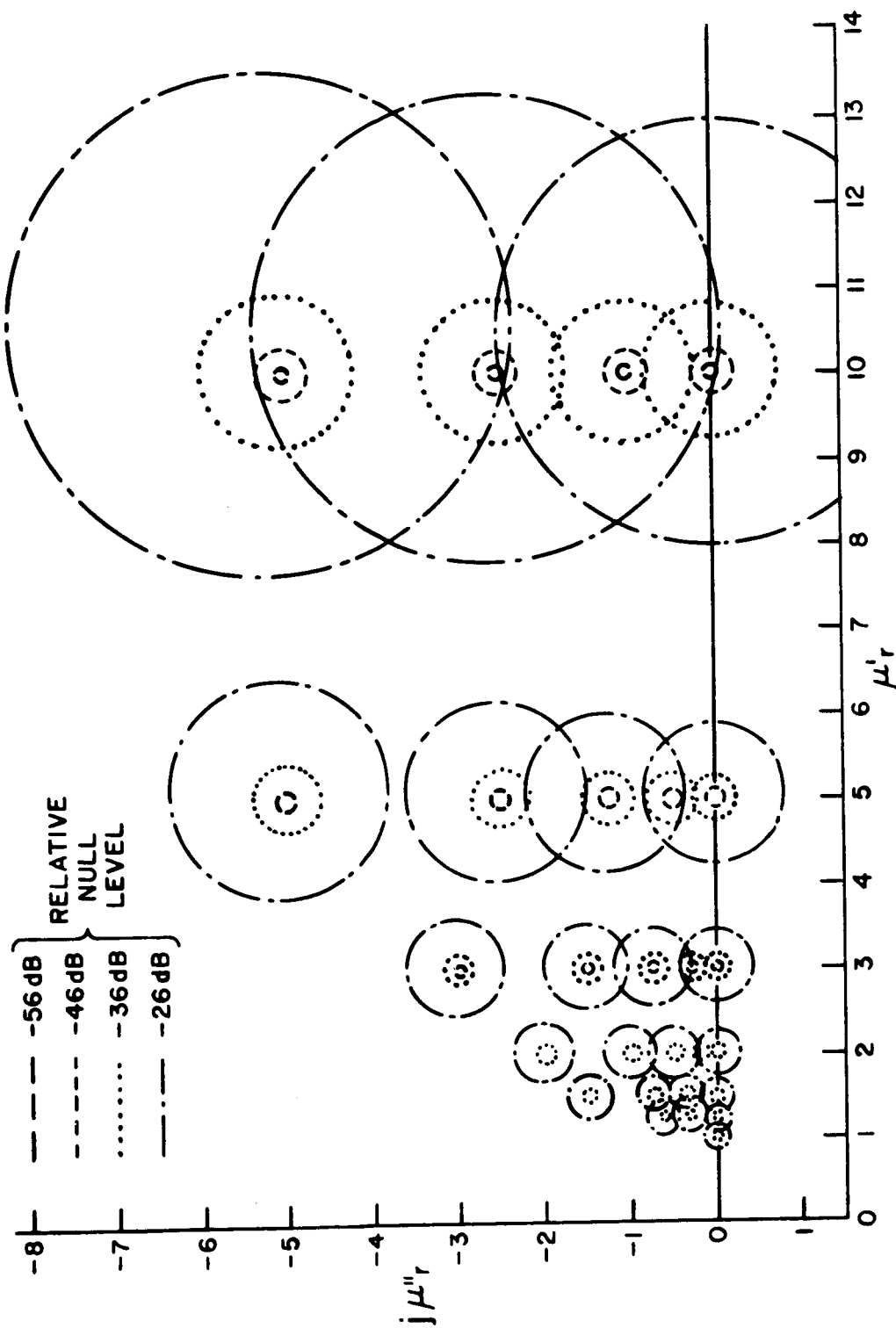


Fig. 14. Locus of possible measured  $\mu_r$  vs. correct  $\mu_r$  and relative null level.

system error signal does have random phase, so that an average of several measurements results in much greater accuracy than can be obtained from a single measurement. Notice however, that the geometric center of the loci, the predicted result of an ideal averaging process, is measurably in error for large  $|\epsilon_r|$  or  $|\mu_r|$  and high null level. The loci in Figs. 13 and 14 also indicate that this method would give high percentage errors in loss tangent or  $\epsilon_r''$  measurement for materials with low loss, for which the magnitude of  $\epsilon_r''$  is comparable to the dimensions of the loci.

In view of the above error analysis, the question must be asked, "Can a practical system be constructed which, using the scattering technique, will measure accurately the constitutive parameters of the rather exotic, complex materials for which it was intended?"

Several factors are involved in the answer to this question. First, considering the probabilities involved, it would seem that maximum possible deviation in  $\gamma$  due to system error would occur very seldom. Measured data seem to verify this assertion. So the realized system should give more accurate results than are guaranteed, without any modifications whatsoever.

Also, as already stated, the system in this report is not considered to have optimum performance. It is estimated that simply by replacing several external components of the system, such as the generator and the null loop components, at least a 10 dB decrease in the null level could be obtained.

Furthermore, sample sphere size could be increased. Using the present theory, valid measurements could be made on spheres of 13/16" diameter at the system frequency. The increased scattered power from these spheres would lower the relative null level approximately 15 dB.

Considering these three factors alone, system performance corresponding to the -56 dB null level seems realizable. Performance equivalent to the -66 dB null level seems feasible if further refinements in temperature stability, physical stability, and other system characteristics were made.

Notwithstanding the feasible performance improvements for this system, the problem of loss tangent accuracy for low-loss materials, which is inherent in this method, as well as others, remains. It is possible that this problem can be greatly reduced by considering a larger spherical target with higher-order modes included so that the measured phase angle is much more sensitive to loss tangent.

Thus, excepting the problem of low-loss tangent measurements, a system does appear to be feasible for measuring accurately the constitutive parameters of materials with constitutive parameters in the range  $1.1 \leq |\epsilon_r| \leq 20$  and  $0.9 \leq |\mu_r| \leq 1.1$  using the simplified scattering method. A system involving four bistatic scattering measurements and using the quadrapole scattering theory would enlarge the range still further, and permit more accurate parameter determination.

## V. SUMMARY AND CONCLUSIONS

A method for determining constitutive parameters of any material at radar frequencies using sphere scattering measurements has been proposed. The practicability of this method depends on the accuracy with which scattering measurements can be made.

A combination transmission line-dipole scattering range for making the required measurements has been built in order to evaluate the experimental problems involved in this technique. Maximum coupling to the sample sphere with minimum direct coupling between antennas was a major goal of the system. Physical stability and electrical isolation were other important characteristics.

Using the above system, measurements have been made at a frequency of 930 MHz on metal spheres of various sizes and sample spheres made of several different materials. Although the measurement results verify the validity of the technique, the accuracy of this system is insufficient for measuring the wide variety of materials proposed. A system error analysis has shown the relationship between constitutive parameter error and an important measure of system quality, the null level relative to metal sphere scattered power. In view of this analysis, some realizable improvements are suggested which would yield a system with satisfactory accuracy. It is therefore concluded that an improved system is feasible for measurements of sufficient quality to render the scattering method practical at this frequency.

Although measurements have not been performed at other frequencies, it is estimated that a scaled system using appropriate circuitry could obtain practical measurements up through S-band frequencies. For higher frequencies, size and tolerance problems might be insurmountable for the simple model. However, the inclusion of higher-order modes in the scattering mechanisms would make it practical to apply the method through the X-band region. Systems operating at frequencies lower than 930 MHz should actually give improved results. The lower frequency limit of

usefulness of this technique is probably set by physical size of the T-line scattering range which should be at least a wavelength in length.

Although the problem of sample preparation has not been fully considered, some general comments on this subject are offered. First, since the dipole scattering modes are relatively insensitive to surface characteristics of the sphere, some degree of surface roughness, as might occur from tumbling, is permissible for the material samples. The magnitude and required symmetry of these perturbations for valid results has not yet been established. Also, since Yu has specified the relation between scattering from metal spheres of different sizes, valid results can be obtained with this method with sample and reference spheres of different size, as long as the sizes are accurately known. Accurate measurement of volume using liquid displacement should be adequate for this purpose.

APPENDIX A  
CIRCUIT COMPONENTS OF THE MEASUREMENT SYSTEM

A. Source

1. Sperry 3K27 klystron, air cooled
2. FXR Type Z815A universal klystron power supply
3. Dymec Frequency Stabilizer  
Stabilizer sensitivity setting:  $< 0.12 \text{ Mc/v}$   
Actual reflector voltage sensitivity of klystron:  $< 0.03 \text{ Mc/v}$

Therefore, greatest possible frequency stabilization was not obtained.

B. Null Loop

1. Hewlett-Packard 393A variable attenuator
2. 2 Sage Model 650 phase shifters

C. Phase Measurement Loop

1. GR 10 dB attenuator
2. Narda Model 230 slab line, crystal diode replaced by shorting plug.

D. Interconnections

1. RG-8U coax cable, type N connectors
2. Sage Model 752 3 dB hybrids
3. Hewlett-Packard Model 765D 20 dB directional coupler
4. Microline Model 157 - impedance transformer

E. Receiver

Scientific Atlanta Series 1600.

## REFERENCES

1. Stratton, Electromagnetic Theory, McGraw-Hill Book Co., New York and London, (1941), pp. 563-567.
2. Yu, Jiunn S., "Determination of the Constitutive Parameters at Microwave Frequencies by the Scattered Fields of a Spherical Body," Report 2148-4, 10 October 1966, Antenna Laboratory, The Ohio State University Research Foundation; prepared under Contract AF 33(615)-3461, Systems Engineering Group, Research and Technology Division, Wright-Patterson Air Force Base, Ohio.
3. Moffatt, D.L., Antenna Laboratory, The Ohio State University, Columbus, Ohio.
4. "Measurement Techniques for Complex Permeability and Permittivity of Highly Conductive Materials at Microwave Frequencies," Progress Report No. 3, May 1966, Emerson and Cuming, Inc., Canton, Massachusetts.
5. Gans, M.J., "Transmission Line Scattering Range," Radar Reflectivity Measurements Symposium, Tech. Doc. Report No. RADC-TDR-64-25, (April 1964) pp. 66-75.